NASA/TM—1999-209077

Aerospace Mechanisms and Tribology Technology: Case Study

K. Miyoshi
Glenn Research Center, Cleveland, Ohio

May 1999

The NASA STI Program Office . . . in Profile

Since its founding, NASA has been dedicated to the advancement of aeronautics and space science. The NASA Scientific and Technical Information (STI) Program Office plays a key part in helping NASA maintain this important role.

The NASA STI Program Office is operated by Langley Research Center, the Lead Center for NASA's scientific and technical information. The NASA STI Program Office provides access to the NASA STI Database, the largest collection of aeronautical and space science STI in the world. The Program Office is also NASA's institutional mechanism for disseminating the results of its research and development activities. These results are published by NASA in the NASA STI Report Series, which includes the following report types:

- TECHNICAL PUBLICATION. Reports of completed research or a major significant phase of research that present the results of NASA programs and include extensive data or theoretical analysis. Includes compilations of significant scientific and technical data and information deemed to be of continuing reference value. NASA's counterpart of peer-reviewed formal professional papers but has less stringent limitations on manuscript length and extent of graphic presentations.

- TECHNICAL MEMORANDUM. Scientific and technical findings that are preliminary or of specialized interest, e.g., quick release reports, working papers, and bibliographies that contain minimal annotation. Does not contain extensive analysis.

- CONTRACTOR REPORT. Scientific and technical findings by NASA-sponsored contractors and grantees.

- CONFERENCE PUBLICATION. Collected papers from scientific and technical conferences, symposia, seminars, or other meetings sponsored or cosponsored by NASA.

- SPECIAL PUBLICATION. Scientific, technical, or historical information from NASA programs, projects, and missions, often concerned with subjects having substantial public interest.

- TECHNICAL TRANSLATION. English-language translations of foreign scientific and technical material pertinent to NASA's mission.

Specialized services that complement the STI Program Office's diverse offerings include creating custom thesauri, building customized data bases, organizing and publishing research results . . . even providing videos.

For more information about the NASA STI Program Office, see the following:

- Access the NASA STI Program Home Page at ***http://www.sti.nasa.gov***

- E-mail your question via the Internet to help@sti.nasa.gov

- Fax your question to the NASA Access Help Desk at (301) 621-0134

- Telephone the NASA Access Help Desk at (301) 621-0390

- Write to:
  NASA Access Help Desk
  NASA Center for AeroSpace Information
  7121 Standard Drive
  Hanover, MD 21076

AEROSPACE MECHANISMS AND TRIBOLOGY TECHNOLOGY: CASE STUDY

Kazuhisa Miyoshi
National Aeronautics and Space Administration
Glenn Research Center
Cleveland, Ohio 44135

INTRODUCTION

In the United States alone a large number of spacecraft failures and anomalies have occurred (e.g., Galileo, Hubble, etc.). In addition, more demanding requirements have been causing failures or anomalies to occur during the qualification testing of future satellites and space platform mechanisms even before they are launched (e.g., GOES–NEXT, CERES, Space Station beta joint gimbals, etc.) (ref. 1). Worldwide a much greater number of failures and anomalies of space mechanisms have occurred. In the operation of space mechanisms functional reliability is, of course, vital. Even a small tribological failure can lead to catastrophic results in a spacecraft (ref. 2).

In this paper a case study is used to review an aspect of a real problem related to vacuum or space tribology technology and dry-film solid lubrication. To understand the adhesion, friction, wear, and lubrication situation, the nature of the problem is analyzed and the tribological properties are examined.

CASE STUDY: GALILEO SPACECRAFT AND HIGH-GAIN ANTENNA DEPLOYMENT ANOMALY

Galileo's Partially Unfurled High-Gain Antenna: The Anomaly at 37 Million Miles

The high-gain antenna for the Galileo spacecraft was built in Florida and shipped by ground transportation to the Jet Propulsion Laboratory (JPL) in California. The antenna was tested and then shipped by ground transportation to the NASA Kennedy Space Center (KSC) in Florida for launch in May 1986. The *Challenger* disaster prevented Galileo from launching in 1986, and so the spacecraft and the antenna were shipped back to JPL and then again returned to KSC for launch in October 1989.

The Galileo spacecraft and its inertial upper stage booster rocket were deployed from the space shuttle *Atlantis* on October 18, 1989. Shortly thereafter, the booster rocket fired and separated, sending Galileo on its six-year journey to the planet Jupiter.

Figure 1 shows the locations of many of Galileo's main structural and scientific components. Galileo is a spin-stabilized spacecraft and has three Earth-to-spacecraft communications antennas for commanding and returning spacecraft telemetry. Two of the antennas are low gain and the third is high gain. The umbrella-like high-gain antenna is located at the top of the spacecraft and is 4.8 m (16 ft) in diameter. It was designed to transmit data back to Earth at rates of up to 134 000 bits of information/sec (the equivalent of about one television picture each minute). The antenna, which is made of gold-plated metal mesh, was stowed behind a Sun shield at launch to avoid heat damage from the direct Sun while the spacecraft flew close to the Sun.

On April 11, 1991, when the Sun-to-spacecraft distance was large enough to present no thermal danger to the antenna, the Galileo spacecraft began to deploy its high-gain antenna under computer-sequence control. Within minutes Galileo's flight team, watching spacecraft telemetry 37 million miles away on Earth, could see that something was wrong: The motors had stalled and something had stuck. The antenna, the 4.8-m mesh paraboloid stretched over 18 umbrella-like ribs, had opened only part way.

Galileo has been in orbit around Jupiter and its moons for the past three years. The spacecraft is operating as it processes and sends science data to Earth with one of the low-gain antennas. The low-gain and high-gain antennas are part of the same assembly and face in the same direction. Its primary mission ended in December 1997, and the spacecraft is currently in the midst of a two-year extension known as the Galileo Europa Mission.

For additional details on Galileo's high-gain antenna deployment anomaly, see references 3 to 5.

Anomaly Investigation

More than 100 people contributed to testing, simulation, analysis, consultation, and review. After a thorough analysis of the telemetry and ground testing and analysis, the investigation attributed the problem to the sticking of 3 of the antenna's 18 ribs in the stowed (or closed) position due to high friction between their standoff pins (locating pins) and their sockets (fig. 2). The other ribs are partially open (fig. 3). The anomaly review team is confident that nothing is broken and that three adjacent antenna ribs are stuck to the central tower by friction in their paired standoff pins, which are likely misaligned enough that one pin binds the upper side of its socket and its mate the lower side (fig. 4).

This attribution led, in turn, to the hypothesis that repeated thermal cycling, warm-cool-warm-cool, could walk the paired pins out, freeing the ribs. The spacecraft was maneuvered to warm the high-gain antenna by solar heating and to cool it in the shade. These warming and cooling cycles, unfortunately, did not release the stuck ribs.

In addition to thermal cycling, other ideas were developed for loosening the stuck ribs, but the antenna still remains stuck. After a multiyear campaign until 1996 to try to free the stuck ribs, there is no longer any significant prospect of deploying the antenna. Although freeing and using the high-gain antenna have not been ruled out, another option has been taken. By using the low-gain antenna, advanced data-compression processing techniques in the spacecraft computers, and advanced hardware and techniques on the ground, a significant fraction of the total planned Jupiter science data has been captured.

Investigation of Adhesion, Friction, Wear, and Cold Welding

Experiment conditions.—To find the causes of stuck antenna ribs in the spacecraft, sliding friction experiments were conducted using a tribometer (vacuum friction apparatus) with a pin-on-disk configuration in space-like vacuum environments and in humid air (ref. 6). The materials, loads, and environments (table I) were chosen to simulate the conditions that the rib-spoke interface of the antenna's locating pins may have experienced.

The contacting surface of the pin specimens was hemispherical with a radius of curvature of 0.5 mm. Two types of pin specimen were examined: coated titanium, 6 wt% aluminum, 4 wt% vanadium (Ti-6Al-4V) alloy pins and bare Ti-6Al-4V alloy pins. The surfaces of the coated Ti-6Al-4V pins were first coated with an electrolytically converted hard coating of titanium, using an all-alkaline bath maintained at room temperature. Then the surfaces of the pins were coated with an inorganic, bonded dry-film lubricant (25 μm thick) that contained a molybdenum disulfide (MoS_2) pigment. The coatings gave antigalling and wear-resistance properties to the surfaces of the Ti-6Al-4V pins (fig. 5). Because the lubricant coating may have failed on the spacecraft, a bare rib-spoke system was also examined as a reference.

The contacting surface of disk specimens was flat, 25 mm in diameter, and 5 mm thick. The disk specimens were uncoated, bare, high-nickel-content superalloy (Inconel 718). The average surface roughness of the disks was 34 nm, root mean square.

Sliding friction in vacuum environment.—

Effect of dry-film lubricant: The coefficient of friction for the dry-film-lubricated Ti-6Al-4V in contact with the bare high-nickel-content superalloy started at 0.23 but rapidly decreased and reached an equilibrium value of about 0.04 (fig. 6(a)). It remained constant at 0.04 for a long period of time. The friction trace fluctuated slightly with no evidence of stick-slip behavior. The sliding action finally caused the coefficient of friction to rapidly increase at 172 370 passes. Wear damage (i.e., local removal of the dry-film lubricant and consequent exposure of the substrate surface), which will be discussed later, caused the high friction at this stage.

The coefficient of friction for the unlubricated, bare Ti-6Al-4V in contact with the bare high-nickel-content superalloy started at 0.31. The friction force traces for the first few sliding passes were characterized by random fluctuation, with only occasional evidence of stick-slip behavior. The presence of oxides and contaminants on the surfaces of the bare Ti-6Al-4V pin and the bare high-nickel-content superalloy disk contributed to the low initial coefficient of friction. Stick-slip behavior became dominant after a few sliding passes. The coefficient of friction rapidly increased with an increase in the number of passes. Also, the higher the number of passes, the greater the stick-slip behavior. At ~10 passes and above, the coefficient of friction reached an equilibrium value of about 1.1 and remained constant for a long period of time (fig. 6(b)). The traces for 10 passes and above were primarily characterized by a continuous, marked stick-slip behavior. This type of friction is anticipated where strong metallic

NASA/TM—1999-209077

Aerospace Mechanisms and Tribology Technology: Case Study

K. Miyoshi
Glenn Research Center, Cleveland, Ohio

National Aeronautics and
Space Administration

Glenn Research Center

May 1999

Available from

NASA Center for Aerospace Information
7121 Standard Drive
Hanover, MD 21076
Price Code: A03

National Technical Information Service
5285 Port Royal Road
Springfield, VA 22100
Price Code: A03

interactions, particularly adhesion, occur at the interface after oxides and contaminants have been removed from the alloy surfaces by sliding action in vacuum.

Comparing figures 6(a) with (b) shows that the adhesion and friction in equilibrium conditions for dry-film-lubricated Ti-6Al-4V were less than those for unlubricated, bare Ti-6Al-4V by a factor of 28. Thus, the dry-film lubricant on the Ti-6Al-4V pin surface was effective and greatly reduced adhesion and friction.

Self-healing of dry-film lubricant.—At 172 370 passes of sliding contact in vacuum (fig. 6(a)) the sliding motion was stopped because of high friction (0.36 or greater) caused by the wear damage. After holding conditions for about 18 hr the sliding was restarted. The result is presented in figure 7(a). The coefficient of friction after restart became much lower than 0.36, generally decreasing to about 0.05 with increasing number of passes. This result suggests that the wear damage occurring in vacuum, which caused high friction at 172 370 passes, can self-heal when rerun in vacuum after a period of hold time.

After 50 passes of sliding contact in the rerun process, the sliding motion was stopped, and the load was decreased from 8.5 to 2.5 N. Contact was maintained for 30 sec and then sliding was begun at the new load. Decreasing the load from 8.5 to 2.5 N did not affect the coefficient of friction, as shown in figure 7(b).

Weakness of MoS_2 Dry-Film Lubricant in Humid Air.—

Sliding friction in humid air : In humid air the coefficient of friction for an MoS_2 dry-film-lubricated Ti-6Al-4V pin sliding on a high-nickel-content superalloy disk started high (~0.30) in the first 23 passes but then decreased to an equilibrium value of about 0.13 (fig. 8). Continued sliding caused the coefficient of friction to increase at 270 passes. When the coefficient of friction then reached an equilibrium value of about 0.32 at 700 passes, the experiment stopped.

When compared with the coefficients of friction obtained in vacuum (fig. 6(a)), the coefficients of friction obtained in humid air (fig. 8) were much greater. The coefficient of friction for the dry-film lubricant in vacuum was one-third of the value in humid air. Further, the endurance life of the dry-film lubricant in vacuum (the number of passes before the onset of a marked increase in friction) was about three orders of magnitude longer than that in humid air.

Seizure when rerun in vacuum: After 700 passes in humid air (fig. 8) the worn surfaces were at rest, and large wear particles loose on the disk surface were blown off. Then the vacuum chamber was evacuated to 10^{-7} Pa. After ~18 hr in contact the sliding motion was restarted. The coefficients of friction, ~0.5, as shown in figure 9(a), for the pin and disk previously worn in humid air were much higher than those (0.05 in fig. 7(a)) for the pin and disk previously worn in vacuum.

After 50 passes of sliding contact in the rerun process the sliding motion was stopped, and the load was decreased from 8.5 to 2.5 N. Contact was maintained for 30 sec and then sliding was begun at the new load. The coefficient of friction continued to increase to 1.4 with increasing number of passes, as shown in figure 9(b). Therefore, seizure between the pin and disk did occur due to wear damage to the dry-film lubricant (i.e., local removal of the dry-film lubricant and exposure of the substrate).

Wear Damage.—

Contact between unlubricated Ti-6Al-4V pin and high-nickel-content superalloy disk: Scanning electron microscopy (SEM) photomicrographs and energy dispersion x-ray analysis (EDX) spectra of the wear damage produced on an unlubricated Ti-6Al-4V pin and on a high-nickel-content superalloy disk after 100 passes at a load of 2.5 N are presented in figures 10 to 13. Figure 10 shows that substantial plastic deformation occurred on the pin. Large wear debris particles formed by plastic deformation and ductile fracture of the Ti-6Al-4V pin are present around the wear scar. Also, plastically deformed grooves and clogged wear debris are present on the wear scar of the pin. Closer SEM examination and EDX analysis of the wear debris showed it to be composed primarily of elements from the Ti-6Al-4V pin (fig. 11) and of small amounts of chromium, iron, and nickel from the disk. Note that abnormally high friction (1.45) was observed when relatively large wear debris clogged the sliding interface.

Figures 12 and 13 show Ti-6Al-4V patches on the wear track of the high-nickel-content disk. The transferred patches occupied a quite large area fraction of the overall wear track. Thus, severe damage, often called scuffing, scoring, or galling, occurred in the contact between the unlubricated Ti-6Al-4V and the high-nickel-content superalloy in vacuum (refs. 3 to 5).

Contact between dry-film-lubricated Ti-6Al-4V pin and high-nickel-content superalloy disk worn in vacuum and rerun in vacuum: SEM photomicrographs of the worn surfaces of a dry-film-lubricated Ti-6Al-4V pin after sliding against a high-nickel-content superalloy disk in vacuum and later rerun in vacuum show surface smearing, tearing, and spalling of the film lubricant (figs. 14 to 17). The wear damage, which resulted from fatigue of the dry-film lubricant, is often called spalling (refs. 3 to 5).

Figure 14(a) shows the relatively smooth burnished surfaces in the upper and lower regions of the wear scar and the rougher surface at the center of the wear scar. Closer SEM examination and EDX analysis of the wear damage at the center of the wear scar showed that the flake-like wear debris (fig. 14(b)) resulted from surface smearing and tearing of the dry-film lubricant. EDX analysis of the flake-like debris indicated that it mainly contained the elements of the MoS_2 lubricant. Figure 14(c) shows a crater (dark area) where fragments of the dry-film lubricant were removed and the Ti-6Al-4V was exposed. The EDX analysis of the crater indicated that it mainly contained elements of the Ti-6Al-4V pin. Interestingly, even with the spalling the extent of removal and fragmentation of the dry-film lubricant was minimal, even though flakes of the dry-film lubricant occupied most of the overall wear scar.

Figures 15 and 16 show a tapered cross section of the worn surface of the dry-film-lubricated Ti-6Al-4V pin at an angle of 45° to the worn surface. The cross-section SEM photomicrographs clearly indicate that most of the dry-film lubricant remained even after ~170 000 passes in vacuum. The film thickness of the remaining lubricant was ~15 μm. Close SEM examination revealed dense, amorphous material in the area right underneath the worn surface (fig. 16(a)).

Figure 17(a) shows the relatively smooth wear track on the high-nickel-content superalloy disk with transferred patches of the dry-film lubricant observed (even in the low-magnification view) mainly at the center of the wear track. Closer SEM examination of the center and upper regions of the track showed the transferred wear particles and patches to be in the form of flakes and powders (figs. 17(b) and (c)).

Contact between dry-film-lubricated Ti-6Al-4V pin and high-nickel-content superalloy disk worn in humid air and rerun in vacuum: SEM photomicrographs and EDX spectra of the worn surfaces of a dry-film-lubricated Ti-6Al-4V pin and a high-nickel-content superalloy disk run in humid air for 700 passes and then rerun in vacuum for 100 passes are shown in figures 18 to 24. Figure 18 shows that both plastic deformation and ductile fracture occurred in the dry-film-lubricated Ti-6Al-4V pin. The backscatter photomicrograph (fig. 18(b)) reveals three different materials: (1) the light areas show where the transferred patches from the disk stayed on the Ti-6Al-4V pin, (2) the grayer areas show the Ti-6Al-4V substrate with no dry-film lubricant present, and (3) the salt-and-pepper areas around the edge of the wear scar show the dry-film lubricant. In addition to the major elements of the disk material the transferred patches also contained elements such as molybdenum and sulfur from the lubricant (fig. 19(a)). On the other hand, the gray areas contained only the elements of Ti-6Al-4V pin (fig. 19(b)).

The large patches on the disk wear track in figure 20(a) are also apparent in the backscatter photomicrograph of figure 20(b), which indicated the dark areas to be the transferred patches from the Ti-6Al-4V pin. Further, EDX analysis (fig. 21(a)) of the transferred patch showed that it mainly contained elements of the Ti-6Al-4V pin with a small amount of elements from the MoS_2 dry-film lubricant. The rest of the areas in the wear track contained relatively smaller amounts of elements from the Ti-6Al-4V pin and the MoS_2 dry-film lubricant (fig. 21(b)). Closer SEM examination (fig. 22) of the wear track revealed extensive plastic shearing of the high-nickel-content superalloy disk.

Figure 23, a tapered cross section of the worn surface of the dry-film-lubricated Ti-6Al-4V pin shows clearly that the dry-film lubricant was not present on the worn surface. Further, in the overview photomicrograph extrusion out of the wear scar and transferred patches of the disk material are also well defined because of effective atomic number contrast. In figure 24 plastic deformation of the Ti-6Al-4V pin (extrusion out of the wear scar) and local solid-state welding (cold welding) between the Ti-6Al-4V pin and transferred patches of the disk material (often called scuffing or scoring) are well defined in the backscatter photomicrographs.

Thus, the worn surfaces of the pin and disk first run in humid air and then rerun in vacuum were completely different from the pin and disk surfaces run only in vacuum. The surfaces worn in humid air (figs. 18 and 20) exhibited galling accompanied by severe surface damage and extensive transfer of the Ti-6Al-4V to the high-nickel-content superalloy disk, or vice versa.

SUMMARY OF RESULTS

The performance of the MoS_2 dry-film lubricant in humid air was poor compared with its performance in vacuum. The coefficient of friction for the dry-film-lubricated system in vacuum was about 0.04, while the value in humid air was 0.13. The endurance life of the dry-film lubricant was about three orders of magnitude longer in vacuum than in humid air.

The worn surfaces of the dry-film-lubricated Ti-6Al-4V pin and high-nickel-content superalloy disk first run in humid air and then rerun in vacuum were completely different from those of the pin and disk run only in vacuum. Galling occurred under the former conditions, whereas spalling occurred under the latter conditions.

When galling occurred in the contact between the dry-film-lubricated Ti-6Al-4V pin and the high-nickel-content superalloy disk first run in humid air and then rerun in vacuum, the coefficient of friction rose to about 0.32 in humid air, to 0.5 at 8.5-N load in vacuum, and to 1.4 at 2.5-N load in vacuum. The galling was accompanied by severe surface damage and extensive transfer of the Ti-6Al-4V to the high-nickel-content superalloy, or vice versa.

When spalling occurred in the dry-film-lubricated Ti-6Al-4V pin run against the high-nickel-content superalloy disk only in vacuum, the coefficient of friction rose to 0.36 or greater. The wear damage, however, self-healed when sliding was stopped and then restarted in vacuum, and the coefficient of friction decreased to 0.05.

CONCLUSIONS

The aforementioned tribological results were also constructively reviewed in Johnson's paper (ref. 5). It is interesting to quote Johnson's conclusion here: "The high contact stress on the V-groove pin/socket interfaces destroyed the integrity of the lubricant film and started the chain of events that led to the deployment anomaly. The use of dry-film lubricant, specifically molybdenum disulfide, on a mechanism that is going to be operated in an atmosphere should be carefully evaluated. The wear rate of the MoS_2 in humid air is so much higher than in a vacuum that any coatings could be worn out by in-air testing and not provide the desired lubrication when needed. The pins and sockets on the high-gain antenna that received the greatest amount of relative motion due to the shipping method were the same ones that were exercised most by the vibration testing. These are also the same pins and sockets that are stuck on the spacecraft. One solution to the problem of ambient testing wearing out the lubricant coating would be to replace the lubricated components just prior to launch so there is a virgin lubricant surface for the flight operation."

As Jost (ref. 2) stated, in the operation of space mechanisms functional reliability is, of course, vital. Even a small tribological failure can clearly lead to catastrophic results. The absence of the required knowledge of tribology can act as a severe brake in the development of new technologies. Tribological reliability of mechanical systems in the highest order will be secured in the operation of many interacting surfaces in relative motion if greater attention (such as the following examples) will be paid to tribology:

1. The effects of adhesion or cold welding on mechanical problems in deep-space vehicles must be determined by performing simulation experiments on various adhesion couples in different environments and temperature ranges.
2. Particular variables contributing to the adhesion process must be scientifically examined before or during technological development and design.

REFERENCES

1. W. Shapiro, et al.: Space Mechanisms Lessons Learned Study, Vol. I: Summary, NASA TM–107046, 1995.
2. H.P. Jost: Tribology—Origin and Future, Wear, vol. 136, 1990, pp. 1–17.
3. J. Wilson: Galileo's Antenna: The Anomaly at 37 Million Miles, Jet Propulsion Laboratory Newspaper, July 3, 1992.
4. Galileo Messenger: Unfurling the HGA's Enigma, Galileo Messenger of Jet Propulsion Laboratory, Aug. 1991.
5. M.R. Johnson: The Galileo High Gain Antenna Deployment Anomaly, 28th Aerospace Mechanisms Symposium, NASA CP–3260, 1994, pp. 359–377.
6. K. Miyoshi, et al.: Properties Data for Opening Galileo's Partially Unfurled Main Antenna, NASA TM–105355, 1992.

TABLE I—EXPERIMENTS

(a) Materials

Contacting materials		Pretreatment		Dry-film lubricant	
Pin	Disk	Pin	Disk	Pin	Disk
Ti-6Al-4V	High-nickel-content superalloy[a]	Bare	Bare	None	None
Ti-6Al-4V	High-nickel-content superalloy[a]	Electrolytically converted hard Ti coating	Bare	Bonded MoS_2 dry-film lubricant	None

(b) Conditions

Load, N	2.5, 4, 8.5
Mean contact pressure, GPa	Approx. 1 to 1.5
Disk rotating speed, rpm	1, 10, and 40
Track diameter, mm	12 to 20
Sliding velocity, mm/s	0.5, 0.9, 8, and 36
Environment:	
Air	40 percent relative humidity
Vacuum	10^{-7} Pa

[a]Composition, wt% (maximum unless shown as range): Ni, 50–55; Cr, 17–21; Fe, 12–23; Nb + Ta, 4.75–5.5; Mo, 2.8–3.3; Co, 1; Ti, 0.65–1.15; Al, 0.2–0.8; Si, 0.35; Mn, 0.35; Cu, 0.3; C, 0.08; S, 0.015; P, 0.015; B, 0.006.

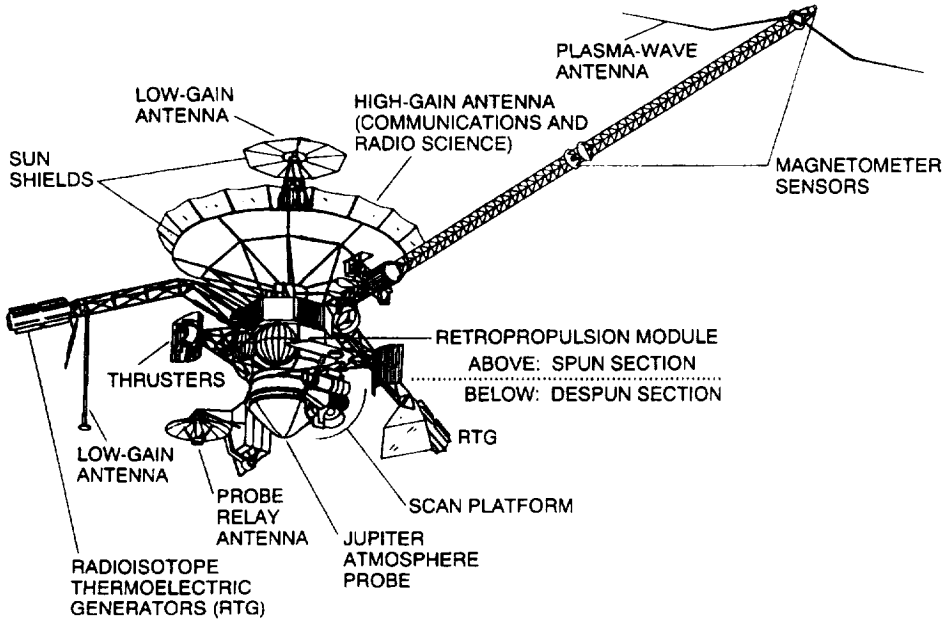

Figure 1.—Galileo spacecraft configuration.

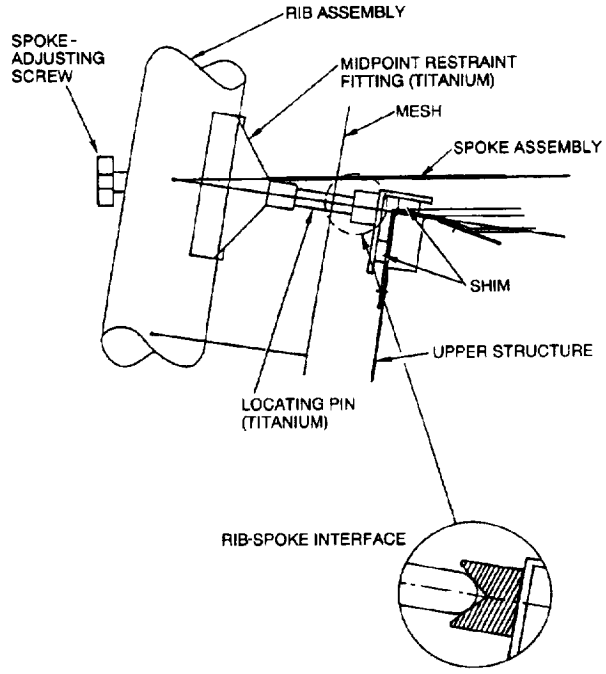

Figure 2.—Rib-spoke interface on Galileo spacecraft high-gain antenna.

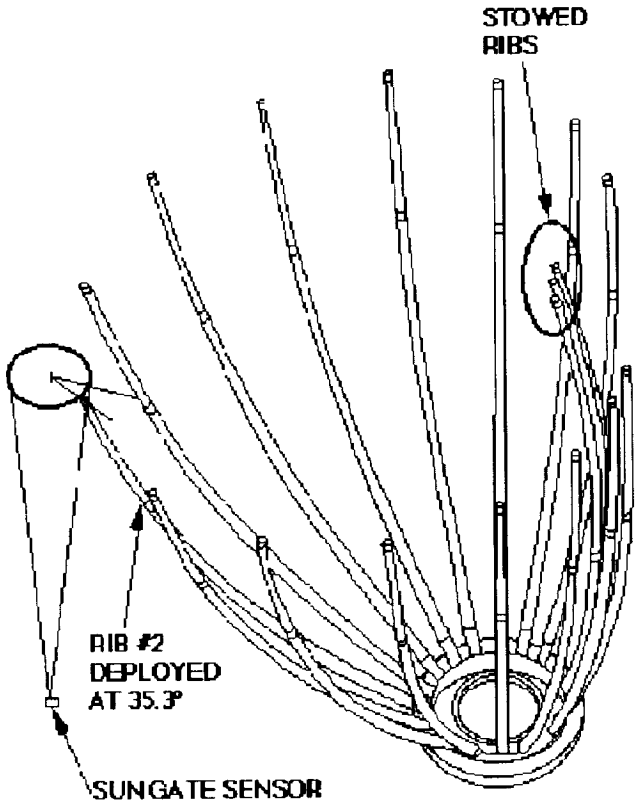

Figure 3.—Ribs of Galileo high-gain antenna, showing three stuck in stowed position.

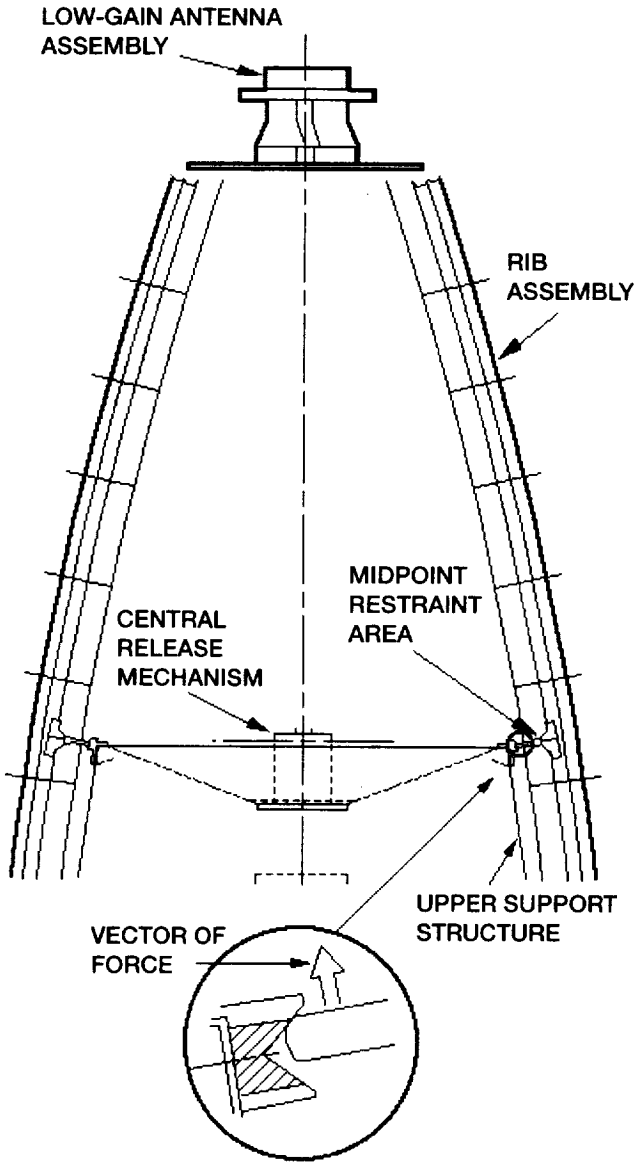

Figure 4.—Standoff pin misaligned in its socket.

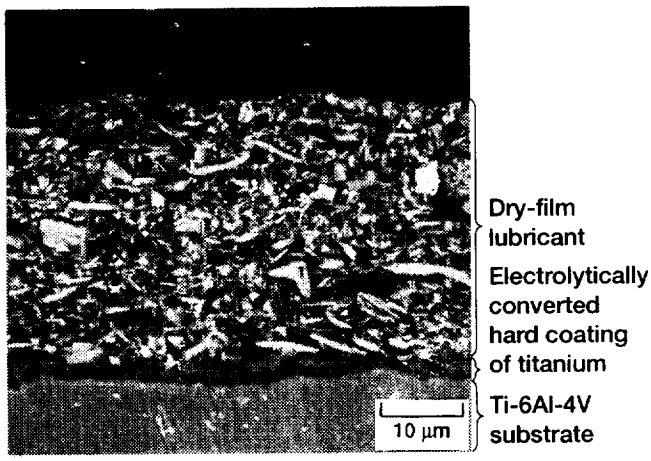

Figure 5.—Tapered cross section of dry-film-lubricated Ti-6Al-4V pin at angle of 45°.

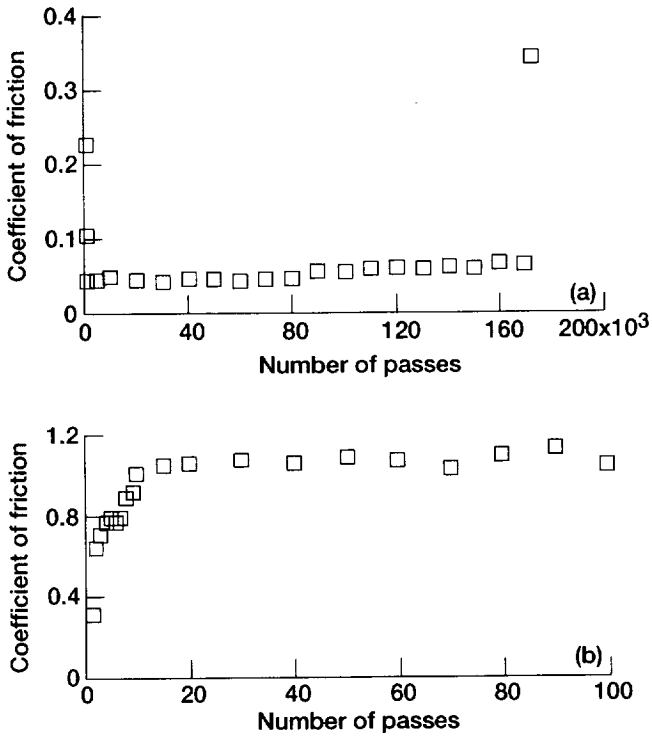

Figure 6.—Coefficients of friction for dry-film-lubricated and unlubricated Ti-6Al-4V pins sliding against high-nickel-content superalloy disks as function of number of passes in vacuum. (a) Dry-film-lubricated pin at 8.5-N load. (b) Unlubricated pin at 4-N load.

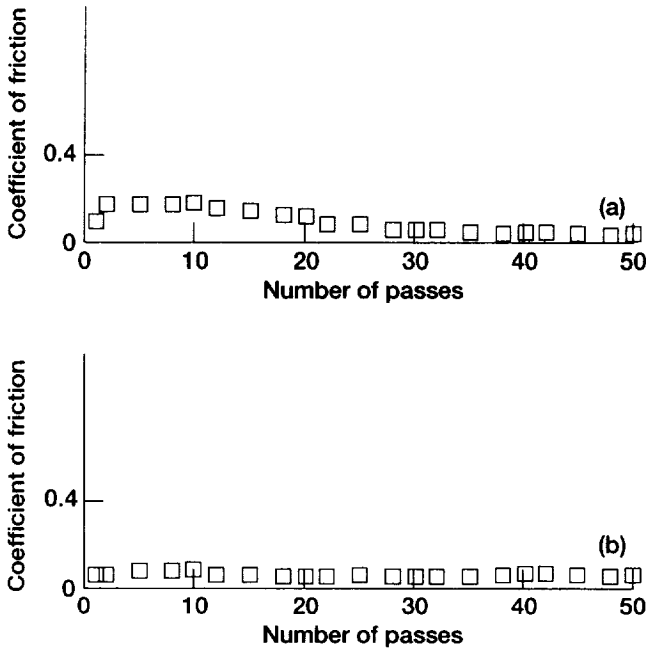

Figure 7.—Coefficients of friction for surfaces previously worn in vacuum of dry-film-lubricated Ti-6Al-4V pin sliding against high-nickel-content superalloy disk as function of number of passes when rerun in vacuum. (a) Load, 8.5 N; rotating speed, 40 rpm. (b) Load, 2.5 N; rotating speed, 1 rpm.

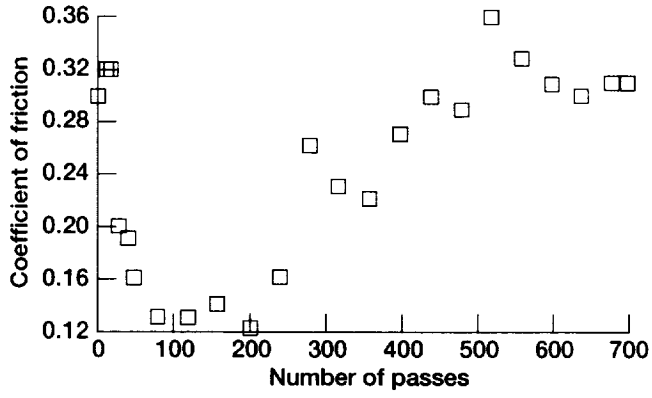

Figure 8.—Coefficients of friction for dry-film-lubricated Ti-6Al-4V pin sliding against high-nickel-content superalloy disk at 8.5 N in humid air as function of number of passes.

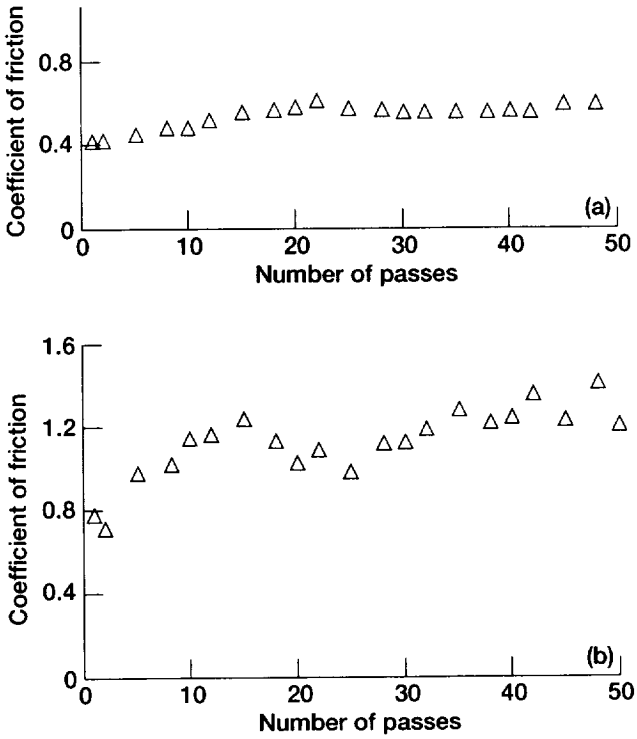

Figure 9.—Coefficients of friction for surfaces previously worn in humid air of dry-film-lubricated Ti-6Al-4V pin sliding against high-nickel-content superalloy disk as function of number of passes when rerun in vacuum. (a) Load, 8.5 N; rotating speed, 40 rpm. (b) Load, 2.5 N; rotating speed, 1 rpm.

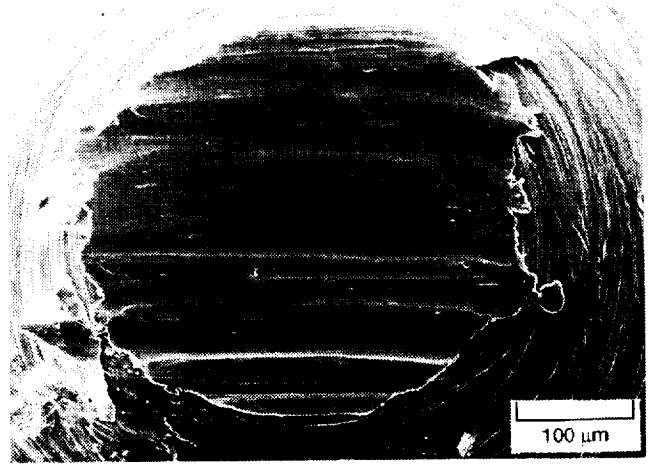

Figure 10.—Wear scar on unlubricated Ti-6Al-4V pin after sliding against high-nickel-content superalloy disk at 2.5 N in vacuum.

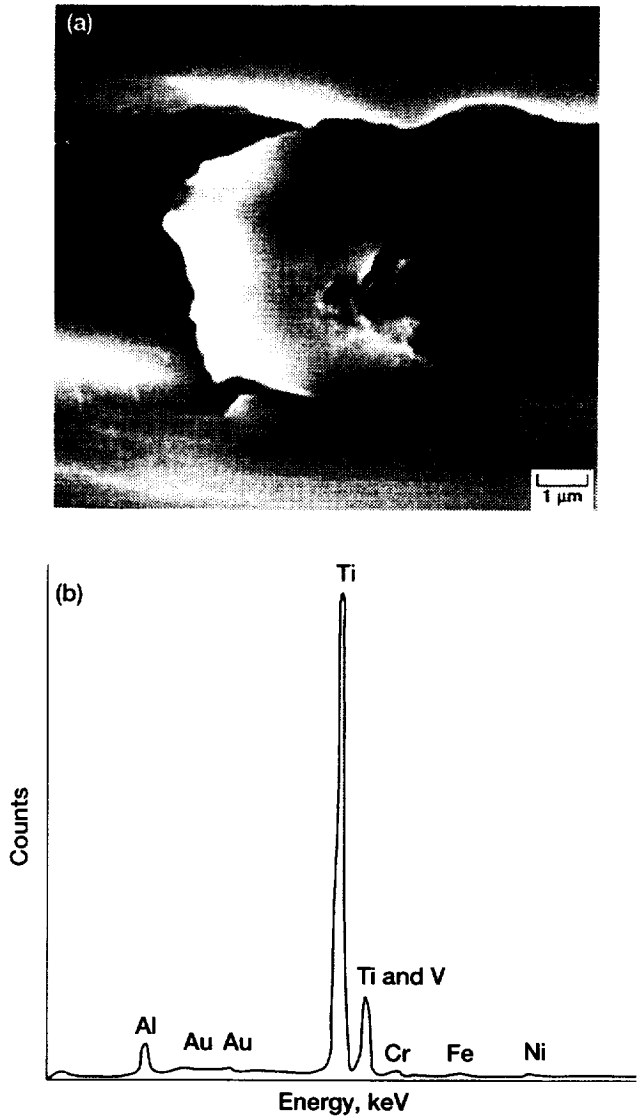

Figure 11.—Clogged wear debris on wear scar on unlubricated Ti-6Al-4V pin after sliding against high-nickel-content superalloy disk at 2.5 N in vacuum. (a) Secondary electron SEM image. (b) Spot EDX analysis. (Thin gold film used to reduce charging of mount is responsible for gold signal in spectrum.)

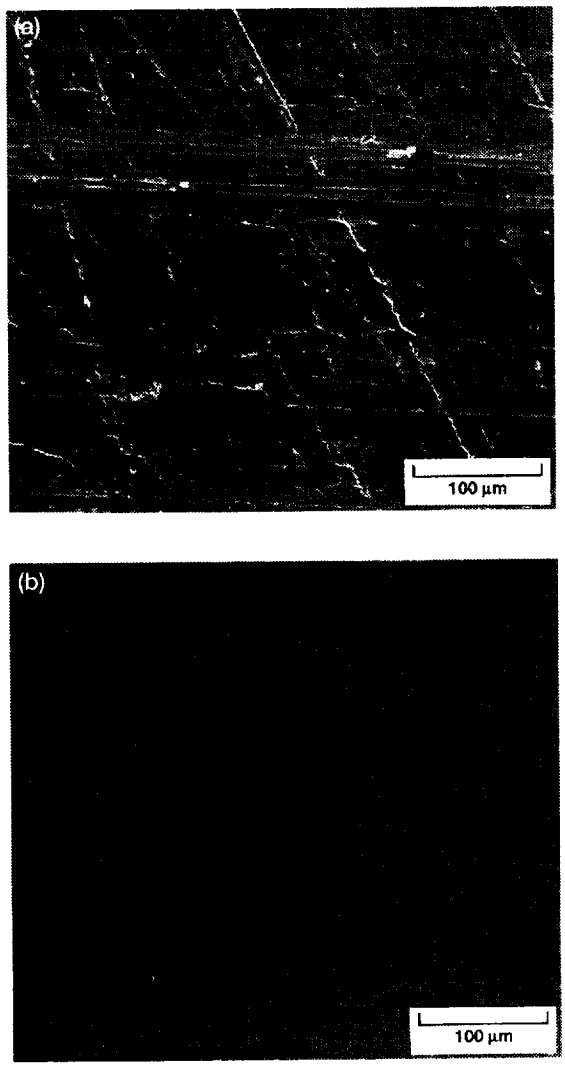

Figure 12.—Wear track on high-nickel-content superalloy disk after sliding by Ti-6Al-4V pin at 2.5 N in vacuum, showing transferred patches of Ti-6Al-4V. (a) Secondary electron SEM image. (b) Backscatter electron SEM image.

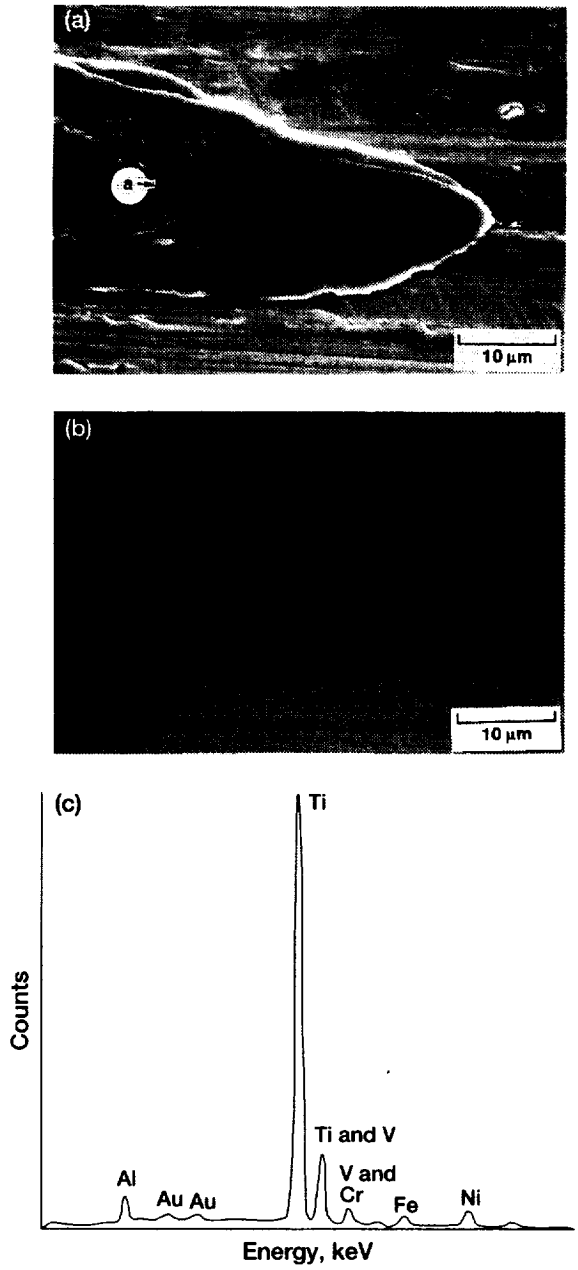

Figure 13.—Large transferred patch of Ti-6Al-4V on high-nickel-content superalloy disk after sliding by Ti-6Al-4V pin at 2.5 N in vacuum, showing transferred patches of Ti-6Al-4V. (a) Secondary electron SEM image. (b) Backscatter electron SEM image. (c) EDX spectrum of transferred film on disk. (Data taken at point indicated in part (a). Thin gold film used to reduce charging of mount is responsible for gold signal in spectrum.)

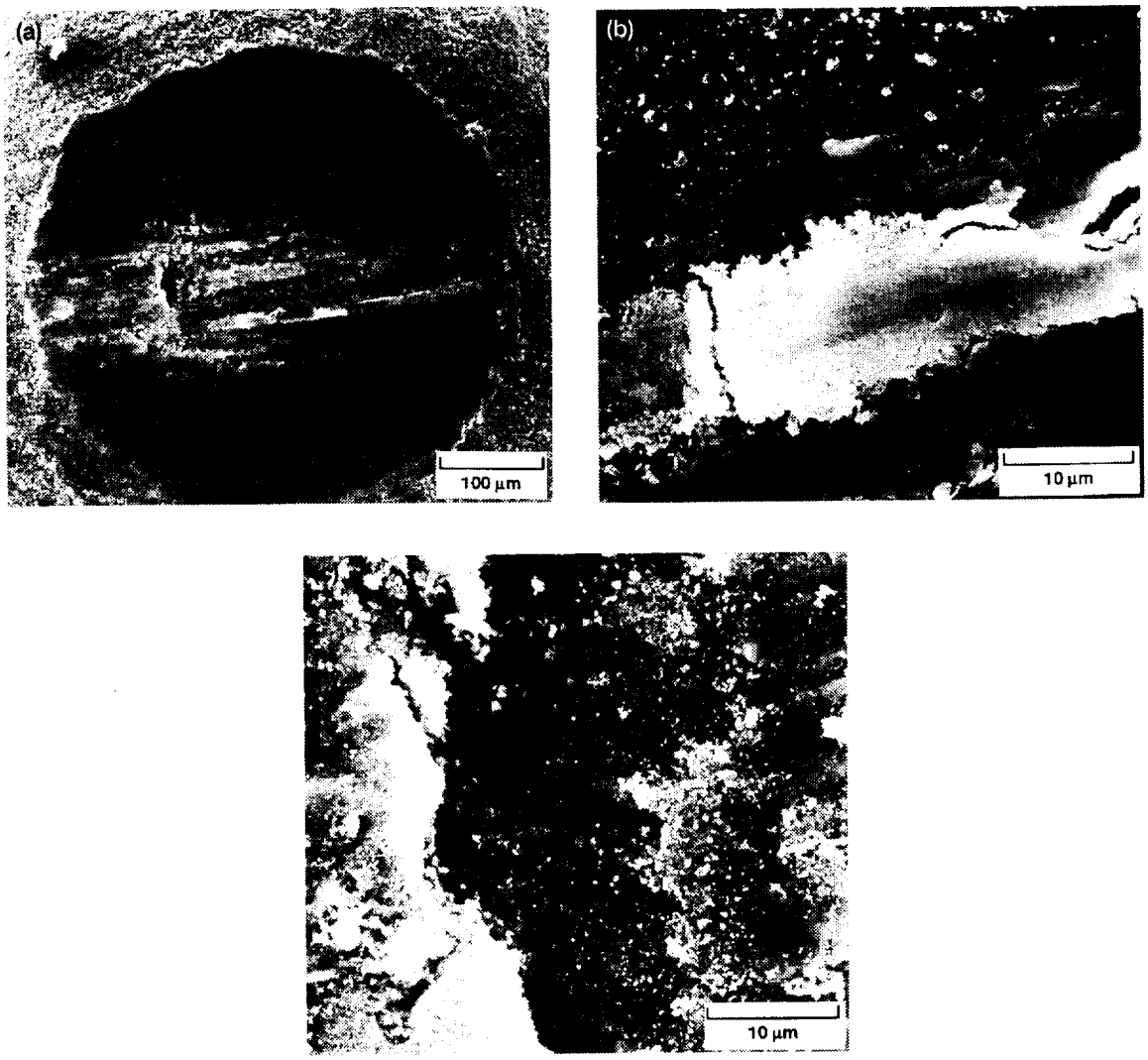

Figure 14.—Wear scar on dry-film-lubricated Ti-6Al-4V pin after sliding against high-nickel-content superalloy disk in vacuum. (a) Low-magnification overview showing relatively smooth surfaces at upper and lower areas with spalling and tearing at center. (b) Surface smearing and tearing at center resulting in particles separating from surface in form of flakes. (c) Spalling at center.

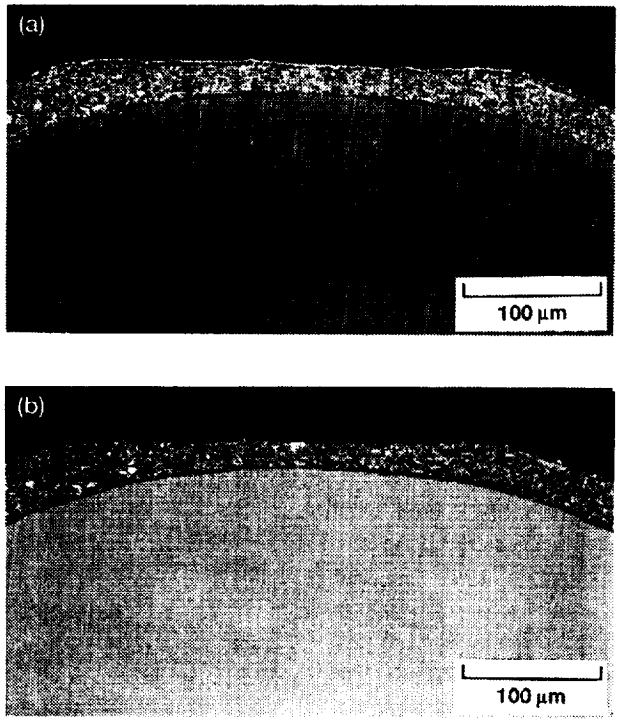

Figure 15.—Tapered cross section of worn surface of dry-film-lubricated Ti-6Al-4V pin at 45° angle to worn surface. (a) Secondary electron SEM image. (b) Backscatter electron SEM image.

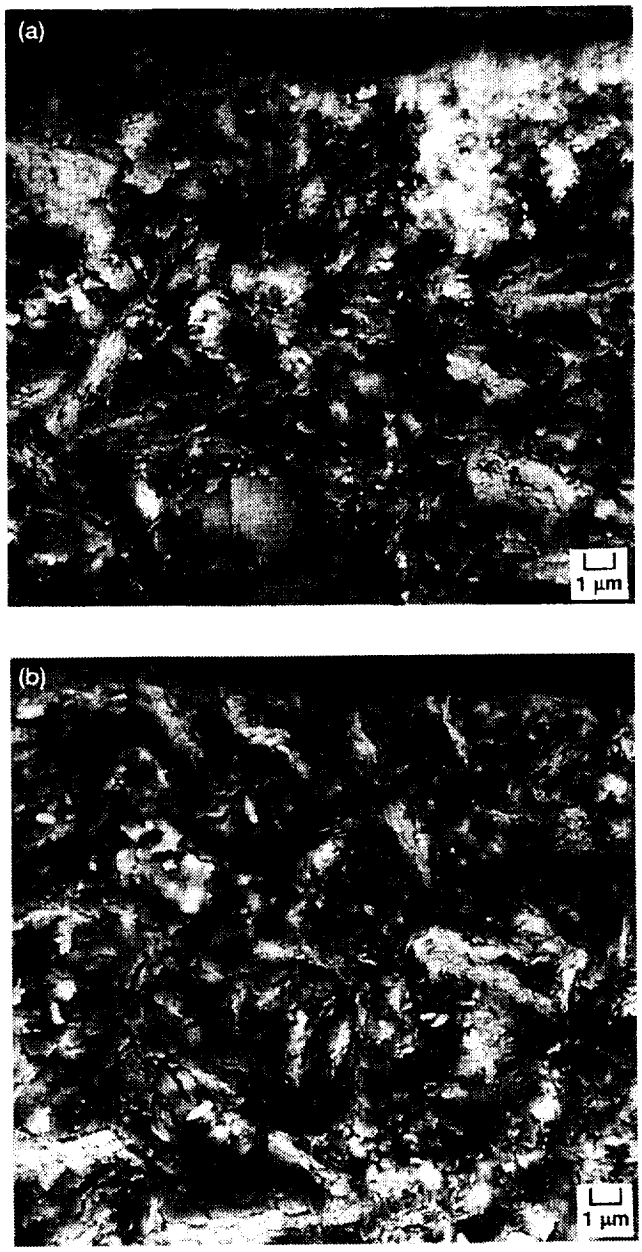

Figure 16.— Backscatter electron SEM image, showing comparison of microstructures. (a) Tapered cross section of worn surface. (b) Tapered cross section of as-coated area of dry-film lubricant.

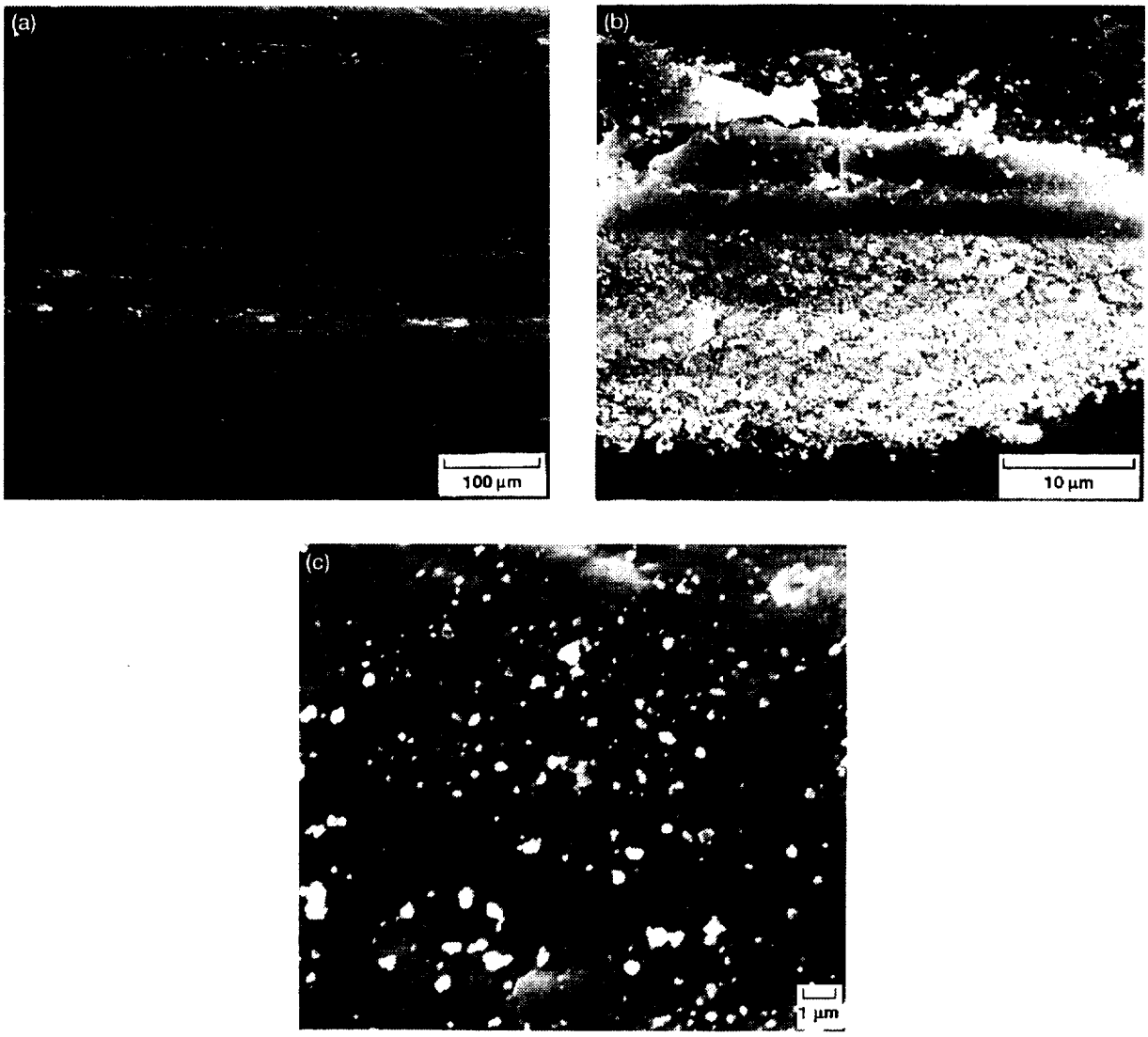

Figure 17.—Wear track on high-nickel-content superalloy disk after sliding by dry-film-lubricated Ti-6Al-4V pin in vacuum. (a) Low-magnification overview. (b) Detailed view showing transferred patches at center. (c) Detailed view showing powder-like wear debris of dry-film lubricant.

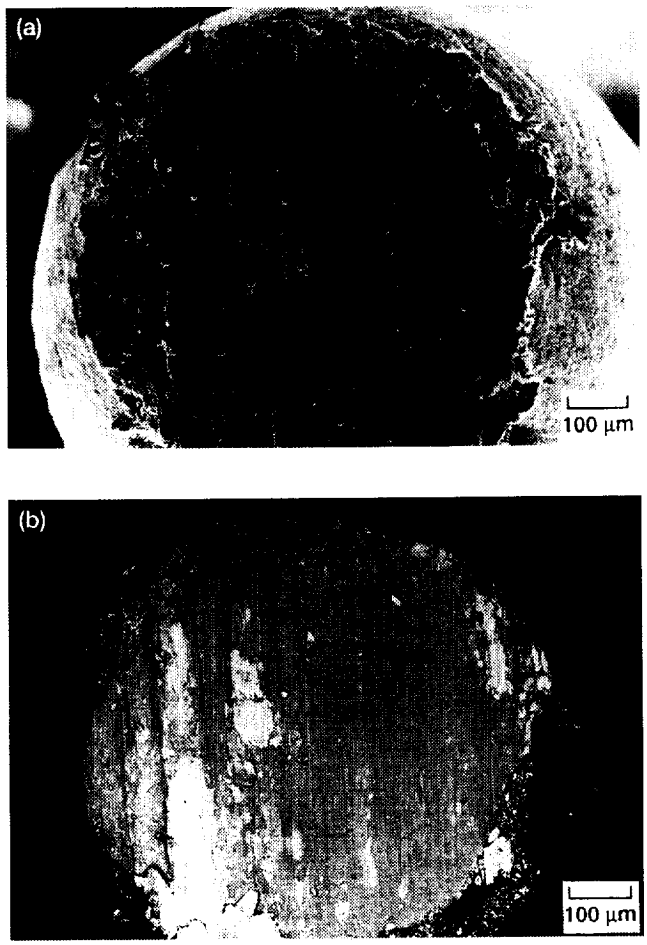

Figure 18.—Wear scar on dry-film-lubricated Ti-6Al-4V pin after sliding against high-nickel-content disk in humid air and then rerun in vacuum.

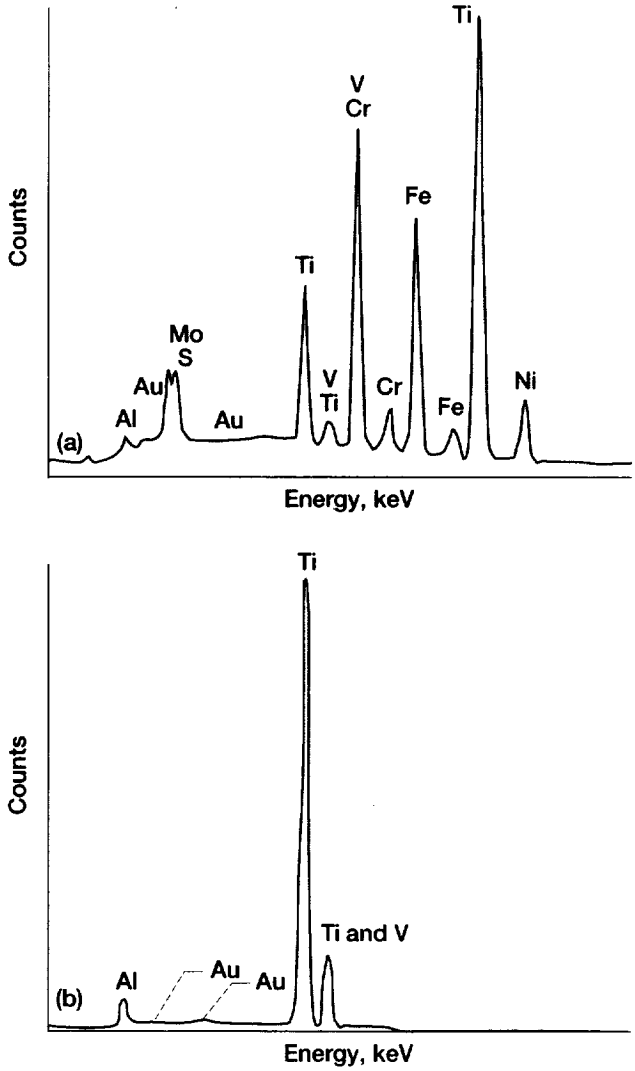

Figure 19.—EDX analysis of wear scar on dry-film-lubricated Ti-6Al-4V pin after sliding against high-nickel-content superalloy disk in humid air and then rerun in vacuum. (Thin gold film used to reduce charging of mount is responsible for gold signal in spectra.)

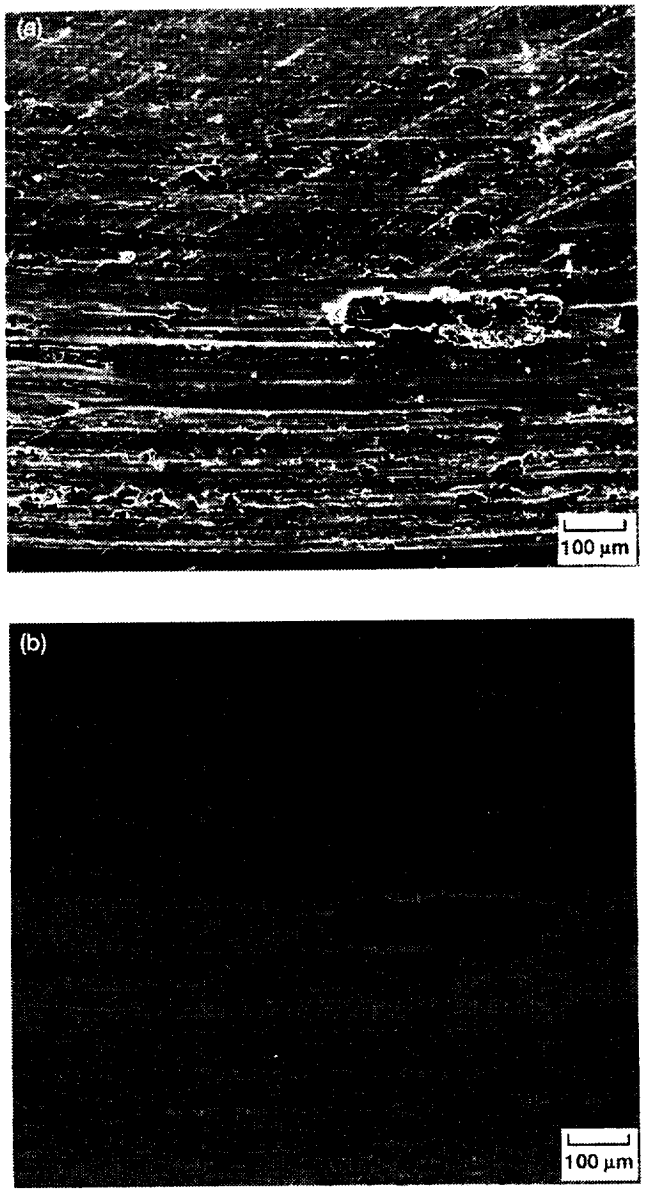

Figure 20.—Wear track on high-nickel-content superalloy disk after sliding by dry-film-lubricated Ti-6Al-4V pin in humid air and then rerun in vacuum.

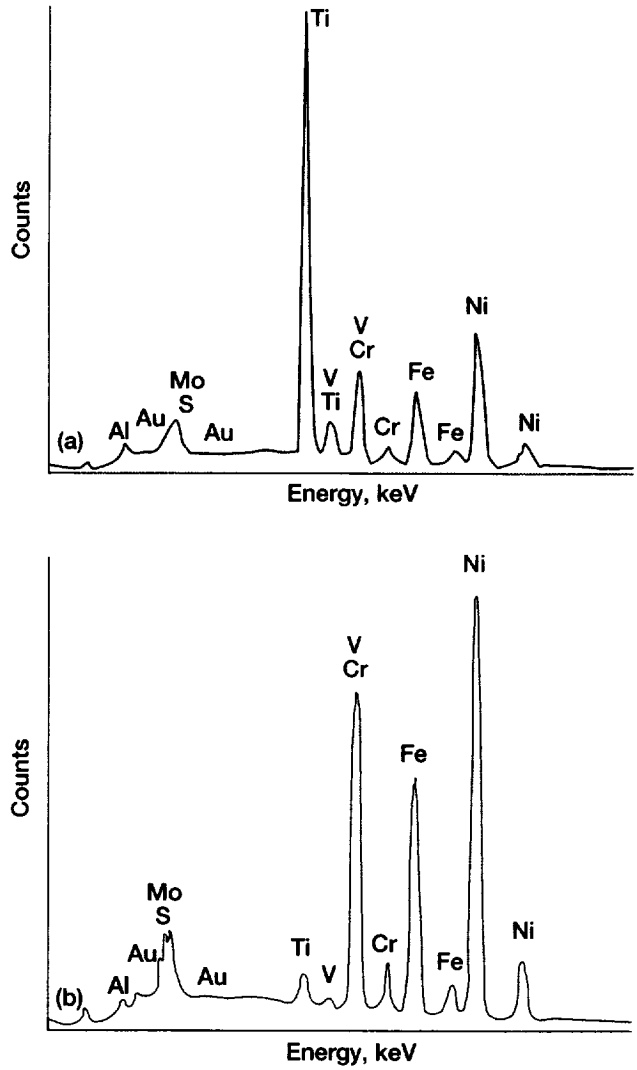

Figure 21.—EDX analysis of wear track on high-nickel-content superalloy disk after sliding by dry-film-lubricated Ti-6Al-4V pin in humid air and then rerun in vacuum. (Thin gold film used to reduce charging of mount is responsible for gold signal in spectra.)

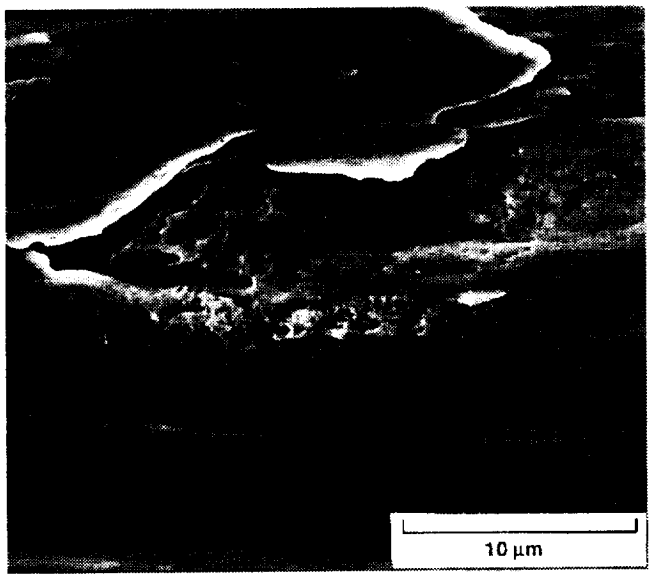

Figure 22.—SEM photomicrograph of wear track showing extensive plastic shearing in high-nickel-content superalloy disk after sliding by dry-film-lubricated Ti-6Al-4V pin in humid air and then rerun in vacuum.

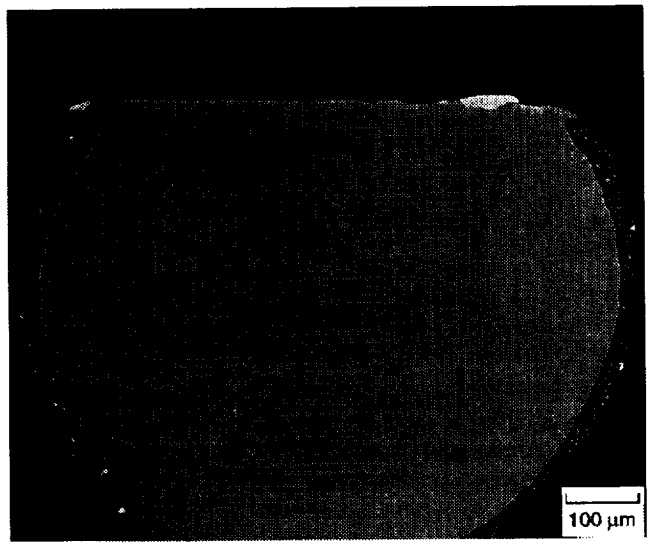

Figure 23.—Overview (backscatter electron SEM image) of tapered cross section at 45° angle to worn surface of dry-film-lubricated Ti-6Al-4V pin after sliding against high-nickel-content superalloy disk in humid air and then rerun in vacuum, showing extrusion out of wear scar, transferred patches of high-nickel-content superalloy, and no dry-film lubricant on worn surface.

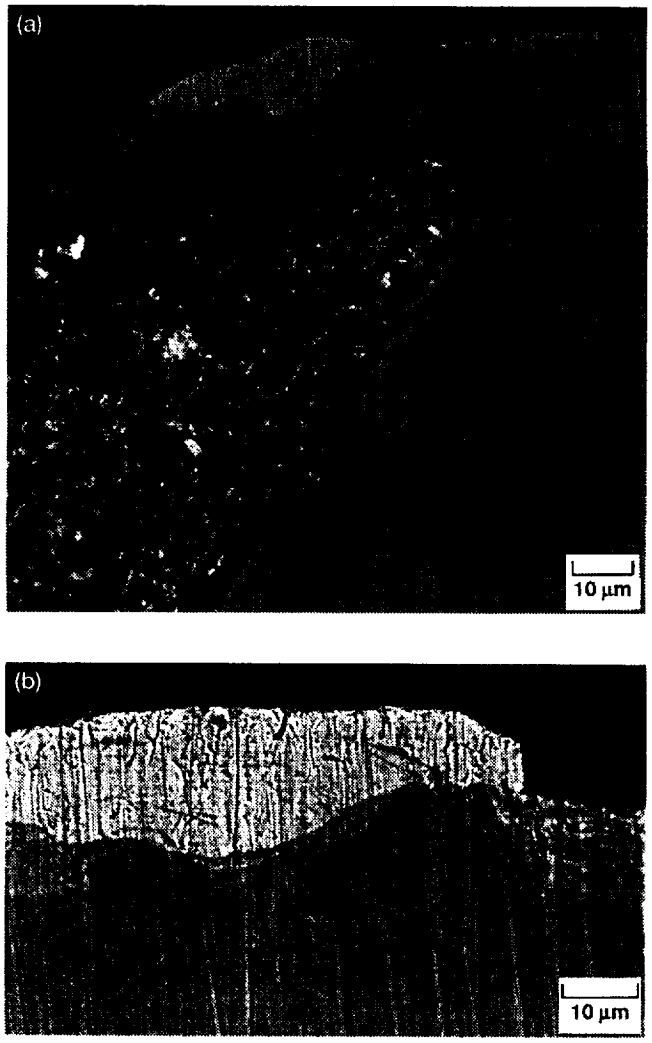

Figure 24.— Backscatter electron SEM images of tapered cross section of worn surface of dry-film-lubricated Ti-6Al-4V pin after sliding against high-nickel-content superalloy disk in humid air and then rerun in vacuum. (a) Showing extrusion out of wear scar. (b) Showing transferred patch of high-nickel-content superalloy on worn surface of dry-film-lubricated Ti-6Al-4V pin.

REPORT DOCUMENTATION PAGE

Form Approved
OMB No. 0704-0188

1. AGENCY USE ONLY (*Leave blank*)	2. REPORT DATE	3. REPORT TYPE AND DATES COVERED
	May 1999	Technical Memorandum

4. TITLE AND SUBTITLE

Aerospace Mechanisms and Tribology Technology: Case Study

5. FUNDING NUMBERS

WU-523-22-13-00

6. AUTHOR(S)

K. Miyoshi

7. PERFORMING ORGANIZATION NAME(S) AND ADDRESS(ES)

National Aeronautics and Space Administration
John H. Glenn Research Center at Lewis Field
Cleveland, Ohio 44135-3191

8. PERFORMING ORGANIZATION REPORT NUMBER

E-11516-1

9. SPONSORING/MONITORING AGENCY NAME(S) AND ADDRESS(ES)

National Aeronautics and Space Administration
Washington, DC 20546-0001

10. SPONSORING/MONITORING AGENCY REPORT NUMBER

NASA TM—1999-209077

11. SUPPLEMENTARY NOTES

Responsible person, K. Miyoshi, organization code 5140, (216) 433-6078.

12a. DISTRIBUTION/AVAILABILITY STATEMENT

Unclassified - Unlimited
Subject Category: 27 Distribution: Nonstandard

This publication is available from the NASA Center for AeroSpace Information, (301) 621-0390.

12b. DISTRIBUTION CODE

13. ABSTRACT ***(Maximum 200 words)***

This paper focuses attention on tribology technology practice related to vacuum tribology. A case study describes an aspect of a real problem in sufficient detail for the engineer and scientist to understand the tribological situation and the failure. The nature of the problem is analyzed and the tribological properties are examined.

14. SUBJECT TERMS

Aerospace mechanisms; Space-vacuum tribology; Solid lubrication

15. NUMBER OF PAGES

30

16. PRICE CODE

A03

17. SECURITY CLASSIFICATION OF REPORT	18. SECURITY CLASSIFICATION OF THIS PAGE	19. SECURITY CLASSIFICATION OF ABSTRACT	20. LIMITATION OF ABSTRACT
Unclassified	Unclassified	Unclassified	